Preprint
September, 2017

Modeling the schizophrenias: subunit-specific NMDAR antagonism dissociates oscillatory signatures of frontal hypofunction and hippocampal hyperfunction

Benjamin Pittman-Polletta[1,2,3]*, Kun Hu[1,2], Bernat Kocsis[1,4]

Abstract
NMDAR antagonism alters mesolimbic, hippocampal, and cortical function, and acutely reproduces the positive, cognitive, and negative symptoms of schizophrenia. Evidence suggests these physiological and behavioral consequences may depend differentially on NMDAR subtype- and region-specific effects. One of the most dramatic electrophysiological signatures of NMDAR blockade in rodents is the potentiation of narrowband high frequency oscillations (HFOs, $\sim$140 Hz) and their phase coupling to θ and δ oscillations. The mechanisms generating HFOs are unknown, but evidence implicates mesolimbic structures, and HFO phase-amplitude coupling (PAC) is related to goal-directed behavior and dopaminergic tone. The goal of this study was to examine the impact of subtype-specific NMDAR antagonism on HFOs and PAC. We found that positive-symptom-associated NR2A-preferring antagonism (NVP-AAM077), but not NR2B-specific antagonism (Ro25-6985) or saline control, replicated abnormal increases in HFO power seen with nonspecific antagonism (MK-801). However, PAC following NR2A-preferring antagonism was distinct from all other conditions. While θ-HFO PAC was prominent or potentiated in other conditions associated with elevated hippocampal θ rhythm, NVP-AAM077 increased δ-HFO PAC and decreased θ-HFO PAC 2-4 hours after administration. δ-HFO PAC was correlated with frontal δ power and θ-HFO PAC was correlated with hippocampal θ power. Furthermore, wake epochs exhibiting narrowband frontal δ oscillations, and not broadband δ characteristic of sleep, selectively exhibited δ-HFO coupling, while paradoxical sleep epochs having a high hippocampal θ/δ ratio selectively exhibited θ-HFO coupling. These results suggest: (1) NR2A-preferring antagonism induces oscillopathies reflecting frontal and subcortical hyperfunction and hippocampal hypofunction; and (2) low-frequency modulation of HFO amplitude may index cortical vs. hippocampal control of mesolimbic circuits.

[1] *Harvard Medical School, Boston, MA*
[2] *Brigham & Women's Hospital, Boston, MA*
[3] *Boston University, Boston, MA*
[4] *Beth Israel Deaconess Medical Center, Boston, MA*
***Corresponding author**: benpolletta@gmail.com

Introduction

NMDA hypofunction is one of the leading hypotheses of schizophrenic pathophysiology [1,2], mainly due to the ability of NMDA receptor (NMDAR) antagonists such as ketamine and phencyclidine to acutely reproduce the positive, cognitive, and negative symptoms of schizophrenia. NMDARs play a variety of roles in different brain structures, making it challenging to understand how NMDA hypofunction impacts different cells, circuits, and systems to bring about its multiple behavioral effects. Indeed, the recent genetic delineation of multiple schizophrenia subtypes [3] suggests that NMDA hypofunction – in its replication of multiple symptom types – may actually model several "schizophrenias" simultaneously. Critical details are missing, however. For example, while several experiments have examined the effects of ketamine on fast and slow oscillations and their phase coupling [4–7], it remains unknown how these changes depend on ketamine's multiple pharmacological actions, including actions on NMDARs, D2 dopamine (DA) receptors, and HCN1 channels [8–10].

A natural way to link molecular changes, such as NMDA hypofunction, to behavioral outcomes, such as schizophrenic symptoms, is to study mesoscale phenomena – signatures of coordinated population activity such as brain rhythms in the electroencephalogram (EEG) & local field potentials (LFP) [11]. Both schizophrenia and NMDAR antagonist drugs induce an array of changes in brain rhythms & their coordination [11–13], and it has been hypothesized that schizophrenia may be mediated by altered rhythmic coordination within & across brain regions [11, 12]. Recently, the study of brain rhythms has provided support for the hypothesis that the mul-

tiplicity of effects of NMDAR antagonism results in part from the heterogeneity of NMDAR subtypes. As hetero-oligomeric complexes, NMDARs consist primarily of two NR1 and two of several types of NR2 subunits. Antagonism of the NR2A receptor subtype, but not antagonism of NR2B, C or D receptor subtypes, has been shown to replicate the changes in γ power seen with positive symptoms in schizophrenia and with non-specific NMDAR antagonists [14]. Thus, NR2A receptor hypofunction may play a key role in mediating schizophrenia's positive symptoms.

One of the most marked and robust oscillatory changes observed with acute NMDAR antagonism in rodents is the potentiation of so-called high-frequency oscillations (HFOs, $\sim$120–160 Hz) [4–7]. These narrowband, highly coherent rhythms are carried by mesolimbic circuits, modulating neuronal firing in the VTA [15] and amygdala [16, 17] as well as current sources and sinks in the nucleus accumbens (NAcc) [18, 19]. HFO amplitude is often modulated by the phase of low-frequency rhythms in the θ ($\sim$6–11 Hz) and δ ($\sim$1–4 Hz) bands. HFO power and coupling are modulated not only by ketamine, but also by sleep state [20, 21], serotonergic [22] and DAergic [10, 23, 24] drugs, the level of cognitive control required by a serial reaction time task [25], the reward probability of a probabilistic reinforcement learning task [26], and fear conditioning and extinction [15, 17]. While their physiological significance remains unknown, these findings suggest that HFOs play a role in the context- and state-dependent deployment of memory and rule-based strategies for goal-directed behavior.

Notably, the mesolimbic θ and δ oscillations that modulate HFO amplitude are driven by rhythmic activity generated in hippocampus [27, 28] and prefrontal cortex (PFC) [29–31], respectively [15, 17]. Evidence indicates that inputs from PFC and hippocampus compete for control over mesolimbic circuits [32–40]. For example, high DA strengthens and potentiates projections from hippocampus to NAcc via its action at D1 receptors while weakening and depressing corticostriatal projections [32–34], and NAcc activity switches its coherence between PFC and hippocampal inputs dependent on task demands [36]. If HFOs predominantly reflect mesolimbic population activity [15–19], their phase modulation may reflect the strength of frequency-specific inputs to mesolimbic circuits, either from cortex at δ frequencies or from hippocampus at θ frequencies. In agreement with this hypothesis, θ-HFO phase-amplitude coupling (PAC) appears to increase in circumstances in which hippocampo-mesolimbic drive is potentiated, such as high levels of cognitive control and high DAergic tone [24, 25], while δ-HFO PAC seems indicative of circumstances in which cortical inputs dominate the mesolimbic system, such as low DAergic tone [24].

While several experiments have examined the effects of ketamine on HFO power and its phase coupling to low frequency oscillations [4–7], fewer studies have used an NMDAR blocker with higher specificity to determine how increases in HFO power depend on ketamine's multiple pharmacological effects [8, 9, 19], and none have examined the possible contributions of NMDAR subtype-specific antagonism to altered HFO activity. Nor, to our knowledge, has the relationship between HFO PAC and cortical and hippocampal oscillations been explored directly. To fill this gap, we examined the effects on rhythmic activity and PAC of three NMDAR antagonists previously shown to differentially affect γ oscillations [14]: nonspecific antagonist MK-801, NR2A-preferring antagonist NVP-AAM077, and NR2B-specific antagonist Ro25-6985. NMDAR antagonism is associated not only with potentiation of HFOs, but also with increased activation of hippocampus [6, 41], increased hippocampal θ [6], disinhibition of prefrontal cortex [42], and altered basal ganglia and mesolimbic function. Thus, our experiments were designed to allow us to observe the coordination between simultaneous changes in HFO power and frontal and hippocampal oscillatory population activity, using simultaneous recordings from frontal cortex, occipital cortex, and hippocampal CA1, while taking advantage of the fact that HFOs are volume conducted from mesolimbic circuits to other brain regions including hippocampus [18] and frontal cortex [19].

We found that MK-801 and NVP-AAM077, in contrast to their comparable effects on γ activity [14] and HFO power, induced markedly different patterns of HFO PAC: while MK-801 potentiated θ-HFO PAC, NVP-AAM077 potentiated δ-HFO PAC and decreased θ-HFO PAC. Indeed, while θ-HFO PAC was plainly visible following all three drugs and in control saline recordings (associated with movement θ), the pattern of δ-HFO PAC seen following NVP-AAM077 injection was not readily observed in other conditions. This striking divergence was paralleled by a dramatic decrease in CA1 θ power following NVP-AAM077 injection. Motivated by findings that a narrowband δ rhythm – distinct from the broadband δ seen during sleep and inactivity – occurs during waking [30, 31], we segregated wake epochs containing narrowband frontal δ in all of our recordings, and found that δ-HFO PAC was selectively associated with narrowband frontal δ as well as clearly discernable, if rare, in all four conditions. Similarly, rapid eye movement sleep (REMS) epochs exhibiting a high θ/δ ratio exhibited high levels of θ-HFO PAC in all four conditions. Finally, examining all conditions and epochs, we found the magnitudes of θ- and δ-HFO coupling to be correlated with frontal δ and CA1 θ power.

Our findings provide evidence for a link between frontal δ oscillations, CA1 θ oscillations, and HFO phase-coupling. They suggest that NR2A-preferring antagonism may potentiate δ oscillations in frontal cortex and inhibit hippocampal θ rhythm, changing the balance of mesolimbic information processing between frontal and hippocampal afferents. These results also suggest that blockade of different NMDAR subtypes may have markedly different effects on the mesoscale physiology of the brain, perhaps resulting in subtype-specific behavioral alterations that may correspond to schizophrenia symptom subtypes and explain the multiple behavioral effects of nonspecific NMDAR antagonism.

1. Methods

1.1 Recordings

Intracranial EEG was recorded from frontal and occipital cortex, and LFP was recorded from hippocampal depth electrodes in six rats, for at least three hours prior to injection, and at least 16 hours following injection. Each rat was injected (on different days with at least 3 days in between) with the NR2A-preferring antagonist NVP, the NR2B-specific antagonist Ro25, the non-specific antagonist MK-801, and saline vehicle as a control. Data were divided into ∼16 s epochs for further analysis.

1.2 Spectral Analyses

Power spectra were calculated for each epoch using the Thompson multitaper method. Power at each frequency was expressed as a percentage of mean baseline power, defined to be the mean power (at a given frequency) over the four hours preceding injection. Measures of power within the δ and θ frequency bands were calculated by summing spectral power over the frequencies within these bands.

1.3 Vigilance States

EMG power and CA1 θ power were used to automatically categorize each epoch into one of three behavioral states: active waking (AW), characterized by high θ and high EMG power; REMS, characterized by high θ power and low EMG power; and quiet waking/non-REM sleep (QW/nREM), characterized by low θ and low EMG power. Candidate REMS epochs were further checked by manual scoring.

1.4 PAC Analyses

PAC comodulograms were computed for all scored epochs. First, oscillations were extracted from each epoch via convolution with 7-cycle complex Morlet wavelets, having central frequencies spaced every 0.25 Hz from 1 to 12 Hz and every 5 Hz from 20 to 200 Hz. Instantaneous amplitude and phase time series $A_f(t)$ and $\phi_f(t)$ were calculated for each frequency f as the absolute value and angle of the resulting complex time series. For each pair of high-frequency amplitude and low-frequency phase time series, an inverse entropy index [43] was computed. The resulting inverse entropy measure (IE) quantifies the degree of phase-amplitude dependence. An IE of zero indicates no phase-amplitude dependence (a uniform distribution of amplitude with respect to phase). An IE of one is obtained when all the amplitude occurs in a single phase bin. In general, higher IE is awarded to distributions exhibiting a stronger dependence of amplitude on phase, including distributions exhibiting multiple peaks.

For a finite data series, IE will always take finite nonzero values, even when no coupling is present in the data. To remove these non-coupling related influences, we used surrogate data to estimate "background" values of IE. These background IE values were estimated using epoch-shuffled surrogate data: for each hour relative to injection in each subject, and for each frequency pair, 1000 random pairings of non-simultaneous high-frequency amplitude and low-frequency phase were used to calculate a distribution of surrogate IE values. For each pair of frequencies, this distribution was used to z-score the observed IE, yielding a z-score of coupling significance or modulation index (MI) for that epoch and pair of frequencies.

1.5 Isolating Epochs of Narrowband Delta

To determine epochs containing narrowband delta, we calculated the entropy of the spectral power in the δ band. The spectrum obtained using the Thompson multitaper method was smoothed by convolution with a Gaussian of standard deviation 0.075 Hz. The smoothed spectrum within the δ range (0.5 – 4.5 Hz) was normalized to have unit sum. The entropy of this distribution of δ power by frequency was computed, resulting in a measure of the uniformity of the distribution of spectral power across frequencies (δ entropy). The higher the δ entropy value, the more uniformly power is distributed across the δ band; the lower the δ entropy value, the "peakier" is the distribution of spectral power in the δ band.

Next, we calculated the values of δ entropy corresponding to the first and last percentile of observed δ entropy across all recorded waking epochs, for each drug. Epochs having a δ entropy less than or equal to the first percentile were considered to exhibit narrowband δ, while epochs having a δ entropy greater than or equal to the last percentile were considered to exhibit broadband δ. Median PAC comodulograms were plotted for these two subsets of epochs.

1.6 Correlating Spectral Power and PAC

To correlate spectral power and PAC, values of MI for all frequency pairs, and values of power in the θ and δ bands, were correlated during the first four hours following injection in all conditions.

1.7 Isolating Epochs with High θ/δ Ratio

To determine epochs containing high θ/δ ratio, we took the ratio of the band power within the θ and δ bands. Within each vigilance state, the epochs having θ/δ ratio within the first and last percentile of observed θ/δ ratios was selected, by the same procedure as for δ entropy, above. Median PAC comodulograms were plotted for these low and high θ/δ ratio epochs.

1.8 Statistics

As IE takes positive values, it is not normally distributed (even after z-scoring against surrogate distributions). This was confirmed using Kolmogorov-Smirnov tests. Thus, median values are used in visualizations, and ranksum tests were used for comparisons to saline. To quantify the similarities and differences in IE between drugs pre- and post-injection, we calculated pairwise ranksum tests (comparing each drug to saline injection) for each six minute period relative to injection. These tests compared the $n = 6$ observations from each rat (averaged over the six minute period) for drug and saline. Tests were performed on sums of IE over frequency ranges of interest. For (baseline-normalized) θ and δ band power,

mean values and standard error are displayed, and t-tests were used for comparisons; otherwise comparisons are as above.

2. Results

2.1 MK-801 and NVP-AAM077 Have Similar Effects on High Frequency Rhythms

Both MK-801 and NVP-AAM077 administration resulted in prolonged periods (∼4–6 hours) of wakefulness and hyperactivity, as opposed to Ro25-6985 and saline. During these periods of wakefulness high γ and HFO power increased dramatically in these two conditions (Fig. 1), roughly following the time course of the abnormal low γ increases reported following these drugs [14, 41, 44]. In contrast, Ro25-6985 did not induce persistent changes in fast oscillations.

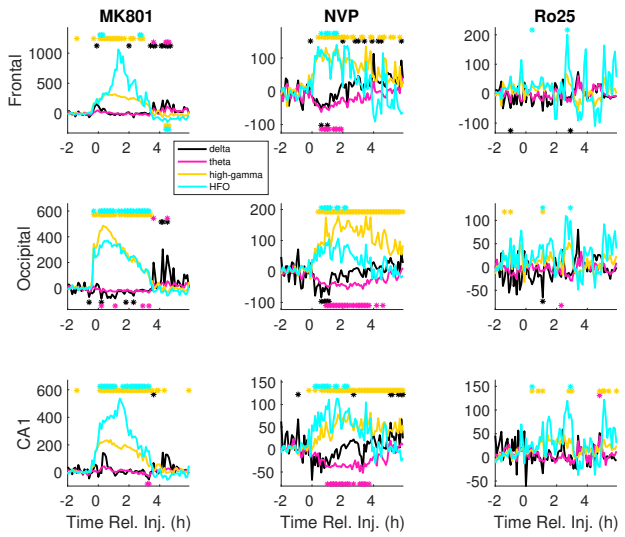

Figure 1. NVP and MK-801 induce similar increases in high frequency power, but have different effects on low frequency power. Median spectral power summed over the δ, θ, high γ, and HFO bands are shown for frontal (top), occipital (middle), and CA1 (bottom) electrodes, following MK-801 (left), NVP-AAM077 (middle), and Ro25-6985 (right) injection. Saline time series have been subtracted off; stars indicate 6 minute periods for which PAC is significantly higher (above) or lower (below) than saline (t-test).

MK-801 and NVP-AAM077 (but not Ro25-6985) also affected slow oscillations. Previous studies [6, 41] reported layer dependent changes in hippocampal θ power after MK-801 administration, with θ decreases in superficial layers of CA1 accompanying strong θ increases in deep electrodes placed at or below the hippocampal fissure. In our current sample, θ showed little change following MK-801 administration, but was strongly suppressed (relative to saline) after NVP-AAM077 administration. This suppression lasted for 4 hours in occipital cortex and CA1, and for 2 hours in frontal cortical recordings. Following NVP-AAM077, power in the δ band showed a biphasic reaction: it was suppressed in the first hour, and then started to rise and reached significantly elevated levels in the frontal cortex during the 3rd to 6th hours post-injection (Fig. 1, middle column). In contrast, δ did not increase following MK-801until 4 hours after injection, when changes in HFO and high γ (and PAC) had worn off.

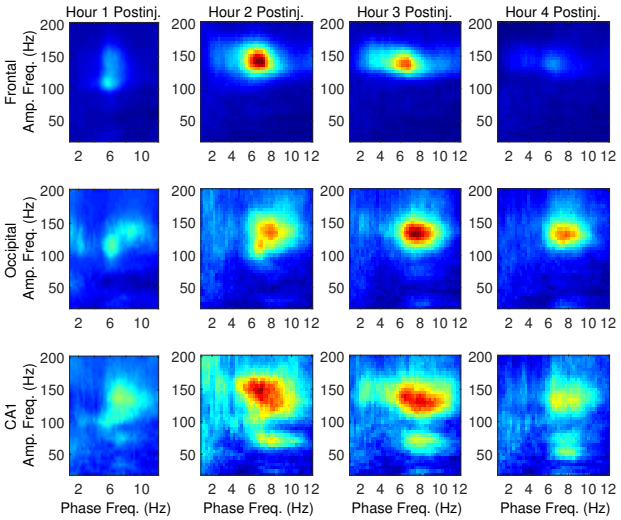

Figure 2. MK-801 increases θ-HFO PAC. Median comodulograms for the first four hours following MK-801 injection, shown for frontal (top), occipital (middle), and CA1 (bottom) electrodes.

2.2 MK-801 and NVP-AAM077 Induce Primarily θ-HFO and δ-HFO PAC, Respectively

In agreement with previous reports for ketamine [5–7], median PAC comodulograms following MK-801 injection revealed dramatic increases in θ-HFO PAC in all brain regions relative to saline injection (Fig. 2), suggesting that ketamine increases PAC through its action at NMDARs, and that its D2 receptor agonism is not necessary for increased coupling. PAC increases were most dramatic in frontal cortex, followed by occipital cortex, and then by CA1. These increases in θ-HFO PAC were accompanied by statistically significant but less dramatic increases in δ-HFO PAC. In CA1, MK-801 injection also led to an increase in θ-γ PAC (Fig. 2).

Following NVP-AAM077 injection, the largest observed effect was an increase in δ-HFO PAC at all sites, relative to saline (Fig. 3). In contrast, only minor increases in θ-HFO PAC were seen in frontal cortex, and decreases in θ-HFO PAC were observed in occipital cortex and CA1, relative to saline (Fig. 4). No changes in θ-γ or δ-γ PAC were observed. This divergence is especially noteworthy, given that NVP-AAM077 is only NR2A-preferring (not strongly NR2A-selective). Following injection of Ro25-6985, few prolonged changes in PAC were observed (not shown).

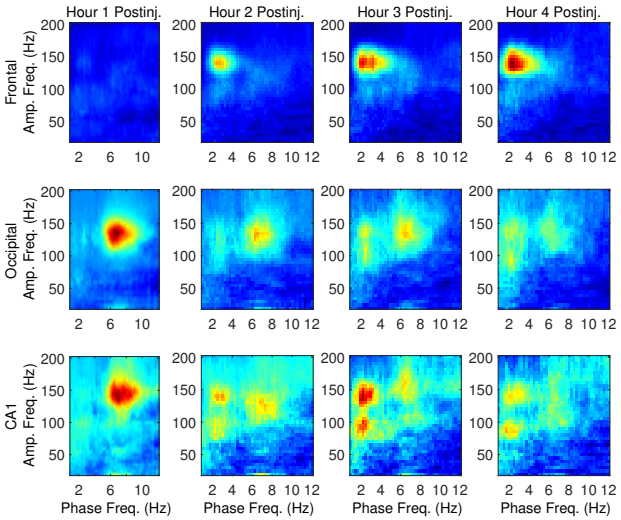

Figure 3. NVP selectively increases δ-HFO PAC. Median comodulograms for the first four hours following NVP-AAM077 injection, shown for frontal (top), occipital (middle), and CA1 (bottom) electrodes.

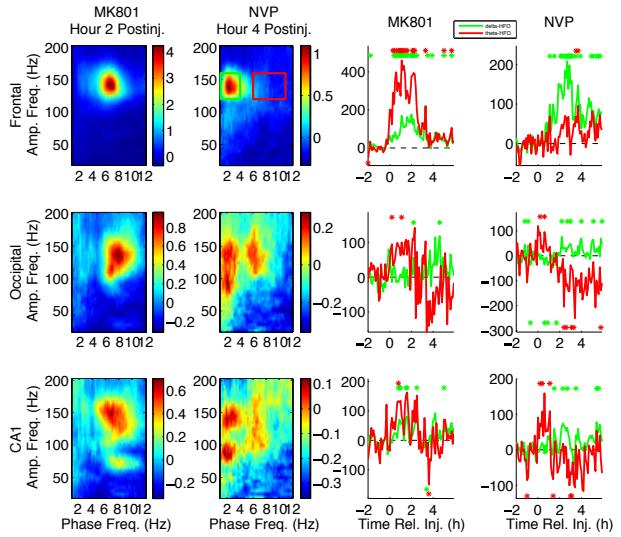

Figure 4. Patterns of phase-amplitude coupling following MK801 and NVP-AAM077 injection differ markedly. Median comodulograms for the hour of largest effect are shown for frontal (top), occipital (middle), and CA1 (bottom) electrodes, following injection of MK-801 and NVP-AAM077 (left two columns), as are timeseries of summed PAC over the θ-HFO (red rectangle) and δ-HFO (green rectangle) ranges (right two columns) from 2 hours pre-injection to 6 hours post-injection. Saline time series have been subtracted off; stars indicate 6 minute periods for which PAC is significantly higher (above) or lower (below) than saline (ranksum test).

Evidence suggests NMDAR antagonist-potentiated HFOs have current generators in mesolimbic circuits, and are then volume conducted to other brain regions [15–19]. However, spontaneous HFOs may be generated locally in other brain regions, including hippocampus [18]. We observed small differences in the time course and spectral parameters of HFO power between recording sites, and differences between sites in HFO PAC, indicating that the predominance of δ and θ oscillations in frontal cortex and CA1, respectively, might bias the detection of δ-HFO PAC in frontal cortex and the detection of θ-HFO PAC in CA1. Thus, for further analyses of the precise timecourse and dynamics of HFO phase modulation, and its correlation with δ and θ power, we utilized only measurements of PAC taken from the "neutral" occipital cortex.

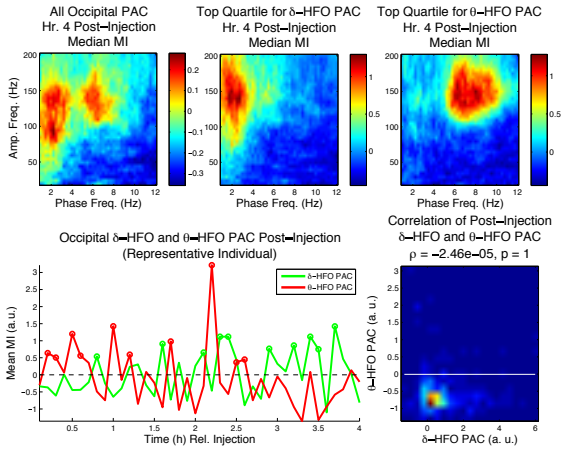

Figure 5. δ-HFO PAC and θ-HFO PAC appear at different times in occipital cortex following NVP-AAM077 administration. The profile of median occipital PAC in the fourth hour following NVP-AAM077 injection (top left) shows both δ-HFO and θ-HFO PAC. However, the profiles of median PAC for the top quartile of epochs with respect to δ-HFO and θ-HFO PAC (top center and right) show that these quantities are separable in time. Time courses of summed δ-HFO and θ-HFO PAC for 6 min. periods following injection (bottom left, representative animal, circles indicate 6 min. periods in the top quartile) show that these two quantities are not correlated. Over all animals, the correlation between δ-HFO PAC and θ-HFO PAC is not significant, with the two variables showing a slightly negative relationship (bottom right).

2.3 Following NVP-AAM077 Injection, δ- and θ-HFO Phase Coupling are Dissociable in Time

To explore the relationship between θ-HFO and δ-HFO PAC appearing in occipital cortex following NVP-AAM077 injection on a short time scale, we examined individual epochs and 6 minute segments of EEG. Figure 5 shows that while the median comodulogram for occipital cortex in the hour of greatest effect following NVP-AAM077 injection (hour 4) shows both θ-HFO and δ-HFO PAC (Fig. 5, top left), the top quartile of epochs for θ-HFO and δ-HFO PAC during hour 4 (Fig. 5, top middle and right) reveal a dissociation between these two phenomena. The representative example in Fig. 5

(bottom left) indicates that the time-courses of δ-HFO and θ-HFO PAC at 6 minute resolution were not positively correlated, and in the four hours following injection, the correlation between δ-HFO PAC and θ-HFO PAC was not significant ($p > 0.05$), though the two variables showed a slightly negative relationship (Fig. 5, bottom right).

In contrast, following MK-801 injection, while the top quartile of epochs for θ-HFO PAC exhibited HFO coupling only to θ frequencies, the top quartile of epochs for δ-HFO PAC exhibited both δ- and θ-HFO PAC, and δ- and θ-HFO PAC were significantly correlated ($p < 10^{-4}$) in the four hours post-injection (Fig. S1). This suggests that the elevation in δ-HFO PAC seen following MK-801 injection is not independent of increased θ-HFO PAC.

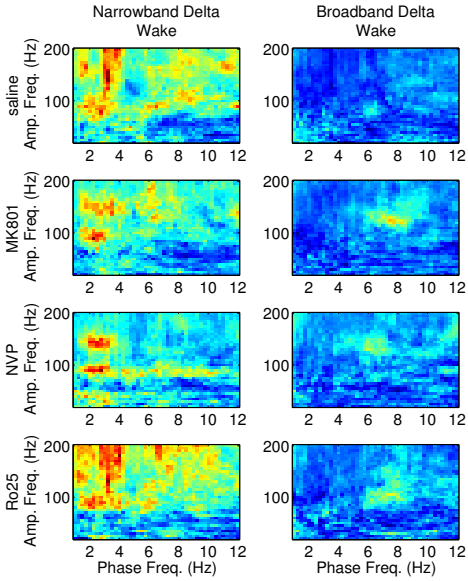

Figure 6. Narrowband frontal δ differentiates wake epochs exhibiting δ-HFO coupling. In all conditions, wake epochs for which the frontal LFP has a narrowband peak in the δ band exhibit δ-HFO coupling (left), while those exhibiting broadband δ do not (right).

2.4 δ-HFO PAC is Restricted to Epochs Containing Narrowband Delta

Since δ power may increase during both sleep and wake, but only wake was seen in the four hours following NVP-AAM077 injection, we hypothesized that the expression of δ-HFO PAC in physiological conditions might depend on the presence of wake-associated narrowband δ oscillations [30, 31]. This waking δ rhythm is different from the broadband δ of slow-wave sleep [30,31], and may be cognitively important [45]. Thus, we sought to hone in on δ-HFO coupling by selecting only those epochs (across all four drugs) in which narrowband δ was observed in frontal electrodes.

To establish that δ oscillations were narrowband, we calculated the entropy of the spectrum within the δ band (treating it as a probability distribution) for the frontal EEG for each epoch (see Methods). The resulting measure of δ entropy quantified the uniformity of spectral power across the δ band. Thus, high δ entropy epochs exhibited broadband δ, while low δ entropy epochs exhibited "peakier", narrowband δ. Over all waking epochs for each drug, we determined the δ entropy values marking the first and last percentiles of observed δ entropy values, and used these to define narrowband and broadband δ epochs, respectively. Figure 6 compares median comodulograms from occipital electrodes for narrowband and broadband δ epochs, for each drug. It shows that δ-HFO PAC is exclusively associated with narrowband δ epochs, and nearly invisible in broadband δ epochs, across conditions.

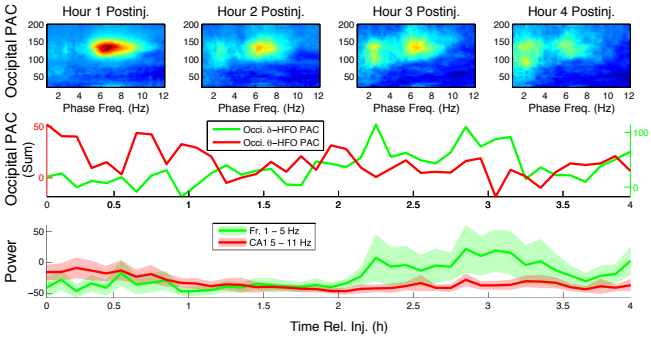

Figure 7. The time courses of frontal δ power and CA1 θ power mirror the time courses of δ-HFO PAC and θ-HFO PAC, respectively. (Top) Profiles of occipital PAC are shown for the first four hours following NVP-AAM077 injection. (Middle) Profiles of median summed PAC (at 6 minute intervals) are shown for δ-HFO and θ-HFO ranges. (Bottom) Frontal δ power (summed over 1–5 Hz) is plotted alongside CA1 θ power (summed over 5–11 Hz).

2.5 θ-HFO and δ-HFO PAC are Correlated with CA1 θ and Frontal δ, Respectively

Figure 7 shows the time-course of δ- and θ-HFO PAC (upper) and its sum over frequency pairs (middle) together with the time evolution of δ and θ power (bottom) in the areas where these slow oscillations most prominently occur and are most likely generated, i.e., in frontal cortex and hippocampal CA1 [27, 28, 30, 31], following NVP-AAM077. Over the same period that HFO phase-coupling switched from θ to δ frequencies, spectral analysis revealed a switch in the relative dominance of CA1 θ power and frontal δ power (Fig. 7, bottom). In contrast, no switch was seen in the relative dominance of CA1 δ and frontal θ (not shown). Comparison of baseline-normalized spectral power in the θ and δ bands between hour 1 and hour 4 post-injection revealed that while frontal δ increased and CA1 θ decreased highly significantly ($p = 0.0198$ and $p = 1.173\text{x}10^{-5}$, respectively), frontal θ and CA1 δ did not change ($p = 0.815$ and $p = 0.931$, respectively).

We hypothesized that these synchronous changes in PAC and spectral power were related. To further establish the connection between CA1 θ and θ-HFO PAC on one hand, and between frontal δ and δ-HFO PAC on the other, we correlated the values of PAC calculated at all frequency pairs with spec-

tral power summed over the δ and θ bands in frontal cortex and CA1, respectively (Fig. S2), at the $\sim$16 second timescale of epochs. This analysis was repeated for all injections, including saline and different NMDAR blockers, and revealed a universal relationship between slow oscillations and HFO modulation. The results show in particular that δ-HFO and δ-high γ PAC were positively correlated, whereas occipital and CA1 θ-HFO PAC were negatively correlated, with frontal δ power (left panels, Fig. S2). In contrast, occipital and CA1 θ-HFO PAC were positively correlated with CA1 θ power, and δ-HFO PAC was negatively correlated with changes in spectral power in the θ band in CA1 (right panels, Fig. S2). This is especially noteworthy given that θ and δ power were either slightly positively correlated (following MK-801, ρ = 0.194 & p = 2.19x10^{-5}; following NVP-AAM077, ρ = 0.217 & p = 2.06x10^{-6}; following Ro25-6985, ρ = 0.111 & p = 0.0152) or uncorrelated (following saline, p = 0.127) in the four hours post-injection.

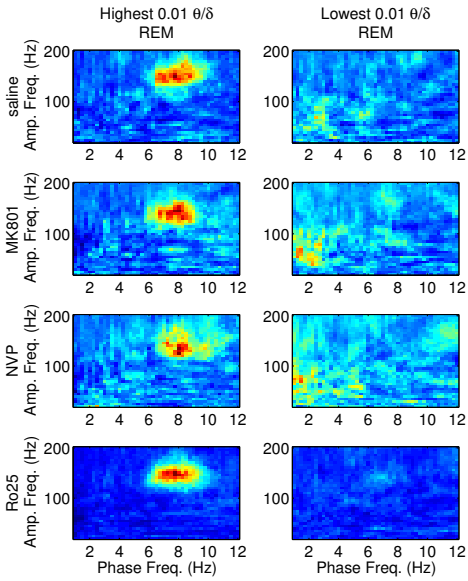

Figure 8. High θ/δ ratio differentiates REMS epochs exhibiting θ-HFO coupling. In all conditions, REMS epochs with a high θ/δ ratio exhibit high θ-HFO coupling (left), while those exhibiting a low θ/δ ratio do not (right).

2.6 θ-HFO PAC is Highest During REMS Epochs Having High θ/δ Ratio

To further probe the dependence of θ-HFO PAC on hippocampal θ, we sought epochs exhibiting high CA1 θ and low frontal δ power. This oscillatory profile is exhibited during REMS, and it has been shown previously that θ-HFO PAC is elevated during REMS relative to both wake and non-REM sleep [21]. We examined the relationship of NMDAR antagonist potentiated θ-HFO PAC to CA1 θ oscillations using the θ state of REMS, and the ratio of CA1 θ power to frontal δ power. Over all REMS epochs for all drugs, we determined the values of the θ/δ ratio marking the first and last percentiles of observed θ/δ ratios, and used these to define low and high θ/δ ratio epochs, respectively. Figure 8 compares median comodulograms from occipital electrodes for high and low θ/δ ratio epochs, for each drug. It shows that θ-HFO PAC is exclusively associated with high θ/δ ratio epochs, and nearly invisible in low θ/δ ratio epochs, across conditions.

3. Discussion

The major findings of this study are that nonspecific NMDAR blockade primarily increased θ-HFO coupling shortly after systemic administration of MK-801, whereas the NMDAR subunit-specific NR2A-preferring antagonist NVP-AAM077 induced a delayed increase in δ-HFO coupling lasting for hours and accompanied by a decrease in θ-HFO coupling. Our observations agree with results on the administration of the non-specific NMDAR antagonist ketamine [4–7, 41]. We show for the first time that changes in HFO phase-coupling following ketamine administration are most likely due to its action on NMDAR and independent of its action at D2 dopamine receptors and HCN1 channels.

Our results allow the formulation of new hypotheses regarding the control and function of mesolimbic circuits. Our observations suggest that subunit-specific changes reflect an association between the dominant frequency of HFO PAC and the power of frontal δ and hippocampal θ oscillations. Following NVP-AAM077 injection, the remarkable predominance of δ-HFO PAC was correlated with frontal δ power, and across conditions, the presence of narrowband δ oscillations characteristic of waking [30, 31] could be used to distinguish epochs exhibiting δ-HFO PAC. On the other hand, θ-HFO PAC was correlated with CA1 θ power, increased during waking locomotion in all conditions, and was observed during REMS epochs exhibiting an elevated ratio of CA1 θ power to frontal δ power.

3.1 HFO Phase Modulation and Control of Mesolimbic Circuits

Multiple pieces of evidence indicate that the HFOs potentiated by NMDAR antagonism and recorded throughout the brain are associated with mesolimbic circuits [15–19], which receive inputs from both frontal cortex and limbic regions including the hippocampus. Given that HFOs reflect the population activity of mesolimbic structures, patterns of HFO PAC may primarily report the dynamic states of these networks. Our results indicate that θ-HFO coupling may be a signature of functional connectivity between hippocampal and mesolimbic networks, while δ-HFO coupling signifies cortico-mesolimbic connectivity. Recent research shows that in frontal-basal ganglia networks, dopamine agonism can switch the frequency of phase modulation of γ and HFO amplitude, from δ to θ [24, 46]. We suggest that one possible mechanism mediating this switch – at least in the case of HFOs – may be the potentiation of hippocampo-accumbal synapses [32–34, 36]. Similarly, the reported state dependence of θ-HFO coupling [21] reflects the predominance of hippocampo-mesolimbic connectivity during REMS.

Behaviorally, hippocampo-accumbal inputs and D1 receptor activation act in concert to enable focus on the current task and execution of the current strategy or action, while cortico-accumbal inputs and D2 receptor inactivation enable flexible switching of focus and strategy [47, 48]. One primary role of the mesolimbic system, and the NAcc in particular, may be to control the switch between flexible and context-driven strategies in goal-directed behavior, something that may be accomplished in part through the selection of cortical vs. hippocampal inputs [47, 48]. Our results suggest that HFO phase-coupling tracks and may even mediate this input selection. Alterations in HFO phase-coupling seen with pharmacological interventions may thus play a key role in the changes in executive function and goal-directed behavior observed with these interventions.

Examining both θ and δ modulation of HFO amplitude is crucial for understanding the functional significance of HFO PAC. In a recent study of human performance on a serial reaction time task [25], NAcc θ-HFO PAC correlated with reaction times, correlated inversely with error rates, and was elevated during task blocks requiring subjects to access newly learned stimulus-response associations ("HCC blocks") relative to task blocks during which subjects repeated a learned motor pattern ("LCC blocks"). These data support the hypothesis that θ-HFO coupling mediates greater focus on task execution by increasing hippocampo-accumbal connectivity. However, the authors speculated that θ-HFO PAC signaled "a deviation from expectancy" implying "the need to stop an automated motor routine" executed during LCC blocks [25]. In contrast, we suggest that LCC blocks represented an HFO PAC-free low-engagement state of habitual responding, while HCC blocks represented a high engagement state of focused task execution. While the authors examined HFO PAC only at phase frequencies above 3 Hz, we suggest that δ-HFO PAC, representing a high engagement state of cortico-mesolimbic drive and strategy re-evaluation, should be observable briefly after shifts from LCC to HCC blocks.

3.2 Subunit-Specific Oscillopathies Dissociate Frontal Disinhibition and Hippocampal Hyperactivity

A large body of research implicates an altered balance between prefrontal and hippocampal activity [11, 49–51] – and its downstream effects on affect, reward, and motivation circuitry [47, 52, 53] – in the pathophysiology of schizophrenia. It has been hypothesized that the selective susceptibility of PV+ inhibitory interneurons to NMDAR blockade may result in the disinhibition of PFC pyramidal cells, and a subsequent increase in "baseline" activity and γ power [11, 54, 55] – a paradoxical case of hyperactivity leading to hypofunction [56]. The increases in high γ and HFO power and in δ-HFO PAC seen in this study with both nonspecific and NR2A-preferring blockade suggest an overlap between the mechanisms generating increased cortical γ power [14] and those generating increased HFO activity. In contrast, the signatures of hippocampal hyperactivity we observed following nonspecific NMDAR blockade – increased θ-HFO PAC and increased hippocampal θ-γ PAC – were absent following NR2A-preferring NMDAR blockade. Indeed, NVP-AAM077 induced a marked decrease in CA1 θ power, suggesting a suppression of hippocampal function. Thus, disinhibition of PFC and hippocampal hyperactivity appear to be dissociable via subunit-specific NMDAR blockade.

The abnormal increases in δ-HFO PAC and HFO power observed following NVP-AAM077 administration may be signatures of prefrontal disinhibition, induced via blockade of NMDARs of NR2A subtype preferentially expressed by PV+ interneurons. The blockade of NMDARs in nucleus reuniens of the thalamus, an important node mediating interactions between PFC and hippocampus [31, 57], also leads to altered prefrontal-hippocampal balance as well as to overexpression of δ rhythms in thalamus and limbic structures [58–62].

It is tempting to hypothesize that the distinct HFO coupling profile observed following NR2A-preferring blockade may contribute to the pathological information processing seen with NVP-AAM077 & MK-801, but not Ro25, administration, through dysfunction of executive control mechanisms. Indeed, our results suggest that the increase in δ-HFO PAC observed following MK-801 injection is not merely a "spectral leakage" artifact of increased θ-HFO PAC, but rather that both θ-HFO and δ-HFO coupling are potentiated by nonspecific NMDAR antagonism, although the expression of increased δ-HFO PAC seems to depend on the concurrent presence of potentiated θ-HFO PAC. Interactions between hippocampal and prefrontal NAcc afferents are abnormal in a developmental model of schizophrenia [47, 53], and an increase in both hippocampo- and cortico-mesolimbic drives, resulting in "focused attention on multiple contingencies", may play a role in the "disrupted focus and ... overwhelming bombardment of stimuli" of schizophrenia [47]. Increased PFC drive to motivational circuits is also hypothesized to be a causal factor in depression [63], and blockade of NR2A-subtype NMDARs may contribute to the acute induction of negative symptoms with NMDAR antagonism. Further exploration of the behavioral effects of subtype-specific NMDAR antagonism will be crucial to testing these hypotheses.

Acknowledgments

This study was supported in part by NSF grant DMS-1042134 (BRPP) and NIH grants HL102241 (KH), AG048108 (KH), MH100820 (BK), and ES006189 (BK).

Supplemental Material

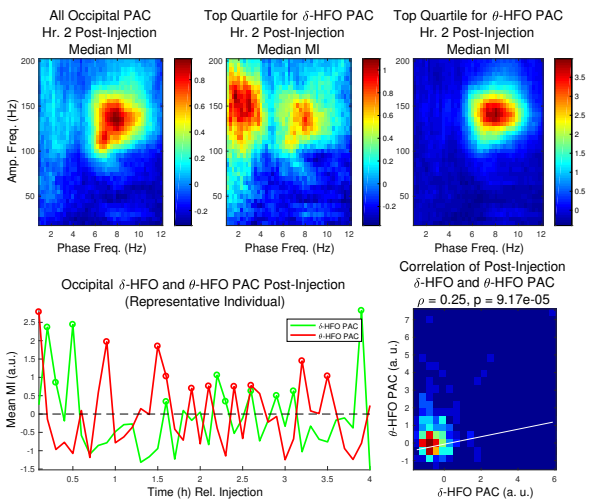

Figure S1. δ-HFO PAC and θ-HFO PAC are correlated in occipital cortex following MK-801 administration. The median occipital comodulograms in the second hour following MK-801 injection (top left) and for the top quartile of epochs with respect to θ-HFO PAC (top right) show primarily θ-HFO PAC. The median comodulogram for the top quartile of epochs with respect to δ-HFO PAC (top middle) shows that δ-HFO PAC co-occurs with θ-HFO PAC. Time courses of summed δ- and θ-HFO PAC for 6 min. periods following injection (representative animal, circles indicate 6 min. periods in the top quartile) appear on the bottom left. Over all animals, there is a significant positive correlation between δ- and θ-HFO PAC (bottom right).

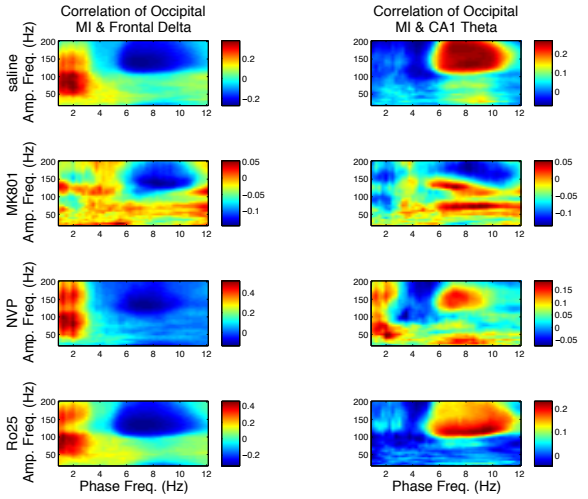

Figure S2. Frontal δ and CA1 θ are correlated with δ-HFO and θ-HFO PAC. The correlation between PAC MI and Frontal δ power (left) or CA1 θ power (right) during the first four hours following injection are shown for each pair of phase-giving and amplitude-giving frequencies, and for each channel, frontal (top), occipital (middle), and CA1 (bottom).

References

[1] John W Olney, John W Newcomer, and Nuri B Farber. NMDA receptor hypofunction model of schizophrenia. *Journal of Psychiatric Research*, 33(6):523–533, 1999.

[2] Albert Adell, Laura Jiménez-Sánchez, Xavier López-Gil, and Tamara Romón. Is the acute nmda receptor hypofunction a valid model of schizophrenia? *Schizophrenia bulletin*, 38(1):9–14, 2011.

[3] Javier Arnedo, Dragan M Svrakic, Coral Del Val, Rocío Romero-Zaliz, Helena Hernández-Cuervo, Molecular Genetics of Schizophrenia Consortium, Ayman H Fanous, Michele T Pato, Carlos N Pato, Gabriel A de Erausquin, et al. Uncovering the hidden risk architecture of the schizophrenias: confirmation in three independent genome-wide association studies. *American Journal of Psychiatry*, 172(2):139–153, 2015.

[4] Mark Jeremy Hunt, Beryl Raynaud, and Rene Garcia. Ketamine dose-dependently induces high-frequency oscillations in the nucleus accumbens in freely moving rats. *Biological psychiatry*, 60(11):1206–1214, 2006.

[5] María Jesús Nicolás, Jon López-Azcárate, Miguel Valencia, Manuel Alegre, Marta Pérez-Alcázar, Jorge Iriarte, and Julio Artieda. Ketamine-induced oscillations in the motor circuit of the rat basal ganglia. *PLoS One*, 6(7):e21814, 2011.

[6] Fábio V Caixeta, Alianda M Cornélio, Robson Scheffer-Teixeira, Sidarta Ribeiro, and Adriano BL Tort. Ketamine alters oscillatory coupling in the hippocampus. *Scientific reports*, 3, 2013.

[7] Ivan Cordon, María Jesús Nicolás, Sandra Arrieta, Eneko Lopetegui, Jon López-Azcárate, Manuel Alegre, Julio Artieda, and Miguel Valencia. Coupling in the cortico-basal ganglia circuit is aberrant in the ketamine model of schizophrenia. *European Neuropsychopharmacology*, 2015.

[8] Xiangdong Chen, Shaofang Shu, and Douglas A Bayliss. Hcn1 channel subunits are a molecular substrate for hypnotic actions of ketamine. *Journal of Neuroscience*, 29(3):600–609, 2009.

[9] MJ Hunt, M Falinska, and S Kasicki. Local injection of mk801 modifies oscillatory activity in the nucleus accumbens in awake rats. *Journal of Psychopharmacology*, 24(6):931–941, 2010.

[10] Maciej Olszewski, Joanna Piasecka, Sailaja A Goda, Stefan Kasicki, and Mark J Hunt. Antipsychotic compounds differentially modulate high-frequency oscillations in the rat nucleus accumbens: a comparison of first-and second-generation drugs. *International Journal of Neuropsychopharmacology*, 16(5):1009–1020, 2013.

[11] Benjamin R Pittman-Polletta, Bernat Kocsis, Sujith Vijayan, Miles A Whittington, and Nancy J Kopell. Brain rhythms connect impaired inhibition to altered cognition

in schizophrenia. *Biological psychiatry*, 77(12):1020–1030, 2015.

[12] Bernat Kocsis, Ritchie E. Brown, Robert W. McCarley, and Mihaly Hajos. Impact of ketamine on neuronal network dynamics: translational modeling of schizophrenia-relevant deficits. *CNS Neuroscience & Therapeutics*, 19(6):437–447, June 2013.

[13] Mark J Hunt and Stefan Kasicki. A systematic review of the effects of NMDA receptor antagonists on oscillatory activity recorded in vivo. *Journal of Psychopharmacology*, 27(11):972–986, 2013.

[14] Bernat Kocsis. Differential role of NR2A and NR2B subunits in N-methyl-D-aspartate receptor antagonist-induced aberrant cortical gamma oscillations. *Biological Psychiatry*, 71(11):987–995, 2012.

[15] AN Serkov and VI Maiorov. δ and θ modulation of fast γ activity in the ventral tegmental area of the midbrain in rats during a conditioned avoidance reflex. *Neuroscience and Behavioral Physiology*, 46(8):957–963, 2016.

[16] Darrell Haufler and Denis Pare. High-frequency oscillations are prominent in the extended amygdala. *Journal of neurophysiology*, 112(1):110–119, 2014.

[17] AN Serkov, VV Serkova, and VI Maiorov. Interaction of the medial prefrontal cortex, ventral hippocampus, and basolateral amygdala during performance of a conditioned avoidance reflex. *Neuroscience and Behavioral Physiology*, 46(7):776–782, 2016.

[18] Mark J Hunt, Monika Falinska, Szymon Lkeski, Daniel K Wójcik, and Stefan Kasicki. Differential effects produced by ketamine on oscillatory activity recorded in the rat hippocampus, dorsal striatum and nucleus accumbens. *Journal of Psychopharmacology*, 25(6):808–821, 2011.

[19] Maciej Olszewski, Wioleta Dolowa, Pawel Matulewicz, Stefan Kasicki, and Mark J Hunt. Nmda receptor antagonist-enhanced high frequency oscillations: Are they generated broadly or regionally specific? *European Neuropsychopharmacology*, 23(12):1795–1805, 2013.

[20] MJ Hunt, P Matulewicz, C Gottesmann, and S Kasicki. State-dependent changes in high-frequency oscillations recorded in the rat nucleus accumbens. *Neuroscience*, 164(2):380–386, 2009.

[21] Claudia Scheffzük, Valeriy I Kukushka, Alexei L Vyssotski, Andreas Draguhn, Adriano BL Tort, and Jurij Brankačk. Selective coupling between theta phase and neocortical fast gamma oscillations during rem-sleep in mice. *PLoS One*, 6(12):e28489, 2011.

[22] Sailaja A Goda, Joanna Piasecka, Maciej Olszewski, Stefan Kasicki, and Mark J Hunt. Serotonergic hallucinogens differentially modify gamma and high frequency oscillations in the rat nucleus accumbens. *Psychopharmacology*, 228(2):271–282, 2013.

[23] Pawel Matulewicz, Stefan Kasicki, and Mark Jeremy Hunt. The effect of dopamine receptor blockade in the rodent nucleus accumbens on local field potential oscillations and motor activity in response to ketamine. *Brain research*, 1366:226–232, 2010.

[24] Jon López-Azcárate, María Jesús Nicolás, Ivan Cordon, Manuel Alegre, Miguel Valencia, and Julio Artieda. Delta-mediated cross-frequency coupling organizes oscillatory activity across the rat cortico-basal ganglia network. *Frontiers in Neural Circuits*, 7:155, October 2013.

[25] Stefan Dürschmid, Tino Zaehle, Klaus Kopitzki, Jürgen Voges, Friedhelm C Schmitt, Hans-Jochen Heinze, Robert T Knight, and Hermann Hinrichs. Phase-amplitude cross-frequency coupling in the human nucleus accumbens tracks action monitoring during cognitive control. *Frontiers in human neuroscience*, 7, 2013.

[26] Satoshi Terada, Susumu Takahashi, and Yoshio Sakurai. Oscillatory interaction between amygdala and hippocampus coordinates behavioral modulation based on reward expectation. *Frontiers in behavioral neuroscience*, 7, 2013.

[27] Robert P Vertes and Bernat Kocsis. Brainstem-diencephalo-septohippocampal systems controlling the theta rhythm of the hippocampus. *Neuroscience*, 81(4):893–926, 1997.

[28] György Buzsáki. Theta oscillations in the hippocampus. *Neuron*, 33(3):325–340, 2002.

[29] Lucy M Carracedo, Henrik Kjeldsen, Leonie Cunnington, Alastair Jenkins, Ian Schofield, Mark O Cunningham, Ceri H Davies, Roger D Traub, and Miles A Whittington. A neocortical delta rhythm facilitates reciprocal interlaminar interactions via nested theta rhythms. *The Journal of Neuroscience*, 33(26):10750–10761, 2013.

[30] Shigeyoshi Fujisawa and György Buzsáki. A 4 hz oscillation adaptively synchronizes prefrontal, vta, and hippocampal activities. *Neuron*, 72(1):153–165, 2011.

[31] Alexis Roy, Frans Pettersson Svensson, Amna Mazeh, and Bernat Kocsis. Prefrontal-hippocampal coupling by theta rhythm and by 2–5 hz oscillation in the delta band: The role of the nucleus reuniens of the thalamus. *Brain Structure and Function*, pages 1–12, 2017.

[32] Patricio O'Donnell and Anthony A Grace. Synaptic interactions among excitatory afferents to nucleus accumbens neurons: hippocampal gating of prefrontal cortical input. *The Journal of Neuroscience*, 15(5):3622–3639, 1995.

[33] Yukiori Goto and Anthony A Grace. Dopamine-dependent interactions between limbic and prefrontal cortical plasticity in the nucleus accumbens: disruption by cocaine sensitization. *Neuron*, 47(2):255–266, 2005.

[34] Yukiori Goto and Anthony A Grace. Limbic and cortical information processing in the nucleus accumbens. *Trends in Neurosciences*, 31(11):552–558, 2008.

[35] Yukiori Goto and Anthony A Grace. Dopaminergic modulation of limbic and cortical drive of nucleus accumbens in goal-directed behavior. *Nature neuroscience*, 8(6):805, 2005.

[36] Aaron J Gruber, Rifat J Hussain, and Patricio O'Donnell. The nucleus accumbens: a switchboard for goal-directed behaviors. *PloS one*, 4(4):e5062, 2009.

[37] Stan B Floresco, Christopher L Todd, and Anthony A Grace. Glutamatergic afferents from the hippocampus to the nucleus accumbens regulate activity of ventral tegmental area dopamine neurons. *Journal of Neuroscience*, 21(13):4915–4922, 2001.

[38] Stan B Floresco, Anthony R West, Brian Ash, Holly Moore, and Anthony A Grace. Afferent modulation of dopamine neuron firing differentially regulates tonic and phasic dopamine transmission. *Nature neuroscience*, 6(9):968, 2003.

[39] Daniel J Lodge and Anthony A Grace. The hippocampus modulates dopamine neuron responsivity by regulating the intensity of phasic neuron activation. *Neuropsychopharmacology*, 31(7):1356, 2006.

[40] Mary H Patton, Brandon T Bizup, and Anthony A Grace. The infralimbic cortex bidirectionally modulates mesolimbic dopamine neuron activity via distinct neural pathways. *Journal of Neuroscience*, 33(43):16865–16873, 2013.

[41] Kara Kittelberger, Elizabeth E Hur, Saba Sazegar, Vidya Keshavan, and Bernat Kocsis. Comparison of the effects of acute and chronic administration of ketamine on hippocampal oscillations: relevance for the NMDA receptor hypofunction model of schizophrenia. *Brain Structure and Function*, 217(2):395–409, 2012.

[42] Houman Homayoun and Bita Moghaddam. NMDA receptor hypofunction produces opposite effects on prefrontal cortex interneurons and pyramidal neurons. *The Journal of Neuroscience*, 27(43):11495–11500, October 2007.

[43] Adriano BL Tort, Robert Komorowski, Howard Eichenbaum, and Nancy Kopell. Measuring phase-amplitude coupling between neuronal oscillations of different frequencies. *Journal of neurophysiology*, 104(2):1195–1210, 2010.

[44] Didier Pinault. N-methyl d-aspartate receptor antagonists ketamine and MK-801 induce wake-related aberrant γ oscillations in the rat neocortex. *Biological Psychiatry*, 63(8):730–735, 2008.

[45] Verónica Nácher, Anders Ledberg, Gustavo Deco, and Ranulfo Romo. Coherent delta-band oscillations between cortical areas correlate with decision making. *Proceedings of the National Academy of Sciences*, 110(37):15085–15090, 2013.

[46] Victoria Andino-Pavlovsky, Annie C Souza, Robson Scheffer-Teixeira, Adriano BL Tort, Roberto Etchenique, and Sidarta Ribeiro. Dopamine modulates delta-gamma phase-amplitude coupling in the prefrontal cortex of behaving rats. *Frontiers in neural circuits*, 11, 2017.

[47] Pauline Belujon, Mary H Patton, and Anthony A Grace. Disruption of prefrontal cortical–hippocampal balance in a developmental model of schizophrenia: reversal by sulpiride. *International Journal of Neuropsychopharmacology*, 16(3):507–512, 2013.

[48] Aaron J Gruber and Robert J McDonald. Context, emotion, and the strategic pursuit of goals: interactions among multiple brain systems controlling motivated behavior. *Frontiers in behavioral neuroscience*, 6, 2012.

[49] Alan Anticevic, Grega Repovs, and Deanna M Barch. Working memory encoding and maintenance deficits in schizophrenia: neural evidence for activation and deactivation abnormalities. *Schizophrenia bulletin*, 39(1):168–178, 2011.

[50] Keith G Phillips, Ullrich Bartsch, Andrew P McCarthy, Dale M Edgar, Mark D Tricklebank, Keith A Wafford, and Matt W Jones. Decoupling of sleep-dependent cortical and hippocampal interactions in a neurodevelopmental model of schizophrenia. *Neuron*, 76(3):526–533, 2012.

[51] Rosalyn J Moran, Matthew W Jones, Anthony J Blockeel, Rick A Adams, Klaas E Stephan, and Karl J Friston. Losing control under ketamine: suppressed cortico-hippocampal drive following acute ketamine in rats. *Neuropsychopharmacology*, 40(2):268, 2015.

[52] Stan B Floresco, Ying Zhang, and Takeshi Enomoto. Neural circuits subserving behavioral flexibility and their relevance to schizophrenia. *Behavioural Brain Research*, 204(2):396–409, 2009.

[53] Pauline Belujon, Mary H Patton, and Anthony A Grace. Role of the prefrontal cortex in altered hippocampal–accumbens synaptic plasticity in a developmental animal model of schizophrenia. *Cerebral cortex*, 24(4):968–977, 2012.

[54] Kevin M. Spencer. The functional consequences of cortical circuit abnormalities on gamma oscillations in schizophrenia: insights from computational modeling. *Frontiers in Human Neuroscience*, 3:33, October 2009.

[55] Monika P Jadi, M Margarita Behrens, and Terrence J Sejnowski. Abnormal gamma oscillations in n-methyl-d-aspartate receptor hypofunction models of schizophrenia. *Biological psychiatry*, 79(9):716–726, 2016.

[56] Aaron J Gruber, Gwendolyn G Calhoon, Igor Shusterman, Geoffrey Schoenbaum, Matthew R Roesch, and Patricio O'Donnell. More is less: a disinhibited prefrontal cortex impairs cognitive flexibility. *Journal of Neuroscience*, 30(50):17102–17110, 2010.

[57] Eric C Zimmerman and Anthony A Grace. The nucleus reuniens of the midline thalamus gates prefrontal-

hippocampal modulation of ventral tegmental area dopamine neuron activity. *Journal of Neuroscience*, 36(34):8977–8984, 2016.

[58] Yuchun Zhang, Rodolfo R Llinas, and John E Lisman. Inhibition of NMDARs in the nucleus reticularis of the thalamus produces delta frequency bursting. *Frontiers in Neural Circuits*, 3, 2009.

[59] Tamás Kiss, William E Hoffmann, and Mihály Hajós. Delta oscillation and short-term plasticity in the rat medial prefrontal cortex: modelling NMDA hypofunction of schizophrenia. *The International Journal of Neuropsychopharmacology*, 14(01):29–42, 2011.

[60] Yuchun Zhang, Takashi Yoshida, Donald B Katz, and John E Lisman. Nmdar antagonist action in thalamus imposes delta oscillations on the hippocampus. *Journal of neurophysiology*, 107(11):3181–3189, 2012.

[61] Yuchun Zhang, Andres Buonanno, Robert P Vertes, Walter B Hoover, and John E Lisman. NR2C in the thalamic reticular nucleus; effects of the NR2C knockout. *PLoS ONE*, 7(7):e41908, 2012.

[62] Aranda R Duan, Carmen Varela, Yuchun Zhang, Yinghua Shen, Lealia Xiong, Matthew A Wilson, and John Lisman. Delta frequency optogenetic stimulation of the thalamic nucleus reuniens is sufficient to produce working memory deficits: relevance to schizophrenia. *Biological psychiatry*, 77(12):1098–1107, 2015.

[63] Anthony A Grace. Dysregulation of the dopamine system in the pathophysiology of schizophrenia and depression. *Nature reviews. Neuroscience*, 17(8):524, 2016.